Improved annular mode variability in a global atmospheric general circulation model with 16 km horizontal resolution

Erool Palipane,[1] Jian Lu,[2] Gang Chen,[3] and James L. Kinter III[1,4]

Received 6 May 2013; revised 7 June 2013; accepted 10 June 2013; published 16 September 2013.

[1] In an attempt to assess the benefit of resolving the subsynoptic to mesoscale processes, the spatial and temporal characteristics of the annular modes (AMs), in particular those related to the troposphere-stratosphere interaction, are evaluated for moderate and high horizontal resolution simulations with the European Centre for Medium-Range Weather Forecast Integrated Forecast System global atmospheric general circulation model in comparison with the reanalysis. Notably, the performance with the high horizontal resolution (T1279 truncation, ~16 km) version of the model is relatively more skillful than the moderate resolution (T159 truncation, ~125 km) on most metrics examined, including the variance of the AMs at different seasons of the year, the intrinsic *e*-folding time scales of the AMs, and the downward influence from the stratosphere to troposphere in the AMs. Moreover, the summer Southern Annular Mode is more persistent in the high resolution and projected to respond in a greater magnitude to climate change forcing than the moderate resolution. **Citation:** Palipane, E., J. Lu, G. Chen, and J. L. Kinter III (2013), Improved annular mode variability in a global atmospheric general circulation model with 16 km horizontal resolution, *Geophys. Res. Lett.*, *40*, 4893–4899, doi:10.1002/grl.50649.

1. Introduction

[2] The Northern and Southern Annular Modes (NAM and SAM) are the dominant patterns of the intrinsic variability of the extratropical circulation in the Northern (NH) and Southern Hemispheres (SH), respectively [e.g., *Thompson and Wallace*, 2000]. The annular modes extend from the surface through the stratosphere in both hemispheres and are characterized by meridional vacillations in the geopotential height field between the polar regions and surrounding latitudes. The annular mode (AM) also describes a pattern of coupling between the stratosphere and troposphere, characterizing the connection between the position of the mid-latitude, eddy-driven jet in the troposphere and the strength of the polar night jet in the stratosphere. *Baldwin and Dunkerton* [1999, 2001] first demonstrated that circulation anomalies originating in the stratosphere can propagate downward and influence the tropospheric circulation for up to 2 months. Thus, the phase of the AM in the stratosphere can be used as a predictor for variations in the troposphere. The tropospheric annular modes tend to be more persistent during the active season of the stratosphere, when the longer time scales of the lower stratosphere may impact the tropospheric persistence. *Baldwin et al*. [2003] quantified the persistence of the AM variability in terms of the *e*-folding time scale of its autocorrelation function. Recent observational evidence suggests that the stratospheric AM index can be a better predictor for the tropospheric variability than the tropospheric one during certain seasons of the year (e.g., SH spring) [*Gerber et al*., 2010].

[3] However, most climate models suffer from biases of (i) overestimating the time scales of the annular modes [*Gerber et al*., 2010; *Baldwin et al*., 2010] and (ii) late breakdown of the polar vortex and hence delay in the peak phase of the AM variances and time scales in both hemispheres. In fact, no climate model previously examined showed skill in capturing the stratospheric predictability for the tropospheric SAM during austral spring. *Gerber et al*. [2008a] found that for a given climate model, higher horizontal resolution tends to alleviate the bias of the overpersistence, and they posited that the lack of sufficient horizontal resolution might be the culprit for the overestimation of the persistence of the AMs in both hemispheres.

[4] An important aspect of the recent and future climate change is the poleward shift of the westerly jet (and correspondingly, the mid-latitude storm track), a change of circulation concomitant with the positive phase of the annular mode [e.g., *Miller et al*., 2006; *Son et al*., 2008]. To the extent that the jet vacillation in latitudes may behave as a fluctuation-dissipation system [*Leith*, 1975], the magnitude of a forced annular mode-like response may scale linearly with the time scale of the intrinsic annular mode variability [*Gerber et al*., 2008a, 2008b; *Ring and Plumb*, 2008; *Chen and Plumb*, 2009]. Therefore, in order to accurately predict future climate change, a general circulation model must correctly simulate the AM time scales and the associated dynamical feedbacks, including that of the downward influence from the stratosphere on the tropospheric time scales.

[5] In a recent multi-institutional, international project—Project Athena [*Kinter et al*., 2013]—the European Centre for Medium-Range Weather Forecast Integrated Forecast System (ECMWF IFS, a weather prediction system) was employed to simulate global climate for multiple decades with multiple horizontal resolutions (ranging from T159, T511, T1279, and T2047 (IFS resolutions are labeled by the triangular truncation wave number of the spectral treatment of the prognostic variables. T159, T511, T1279, and T2047

[1]Department of Atmospheric, Oceanic and Earth Sciences, George Mason University, Fairfax, Virginia, USA.
[2]Pacific Northwest National Laboratory, Richland, Washington, USA.
[3]Department of Atmospheric and Earth Sciences, Cornell University, Ithaca, New York, USA.
[4]Center for Ocean-Land-Atmosphere Studies, Institute of Global Environmental and Society, Fairfax, Virginia, USA.

Corresponding author: J. Lu, Pacific Northwest National Laboratory, 902 Battelle Boulevard, P.O. Box 999, Richland, WA 99352, USA. (jian.lu@pnnl.gov)

©2013. The Authors.
This is an open access article under the terms of the Creative Commons Attribution-NonCommercial-NoDerivs License, which permits use and distribution in any medium, provided the original work is properly cited, the use is non-commercial and no modifications or adaptations are made.
0094-8276/13/10.1002/grl.50649

The copyright line for this article was changed on 30 MAR 2015 after original online publication.

correspond to 125, 39, 16, and 10 km grid spacing, respectively), allowing a comparison of climate simulations with minimal differences in model configuration aside from horizontal resolution. Studies of the Athena project have already shown that increasing the model resolution improves the representation of tropical cyclones [*Manganello et al*., 2012], extratropical cyclones and blocking [*Jung et al*., 2011], and the diurnal cycle of precipitation [*Dirmeyer et al*., 2011]. In view of the improvements above and the fact that the mean wind speed in the T1279 resolution has better agreement with the observation relative to the T159 simulation (not shown), we set out to further assess how the benefit of the very high horizontal resolution would be manifested in the time scales and the potential predictability of the AMs. Since future climate simulations were also conducted in the form of time-slice experiments, the resolution with better fidelity in representing the key characteristics of the internal variability of the AMs may be assigned higher confidence in its projection of the AMs under a warmed climate.

[6] In this letter, we will first introduce the data and methods used. The analysis will be centered around examining the basic temporal and spatial structure of the AM variability, its variance in time and space, and how the representation of the AMs in the stratosphere may impact the seasonality in the tropospheric AM variability. Further, we will show that the enhanced SAM time scales during austral summer seem to be manifested in the climate change simulation of the SH westerly jet shift. Lastly, we will summarize the findings of this study and speculate on the possible cause for the improvements in the high-resolution simulations of the IFS.

2. Data and Methods

[7] Two types of simulations—Atmospheric Model Intercomparison Project (AMIP)-type and time-slice experiments—are conducted with the IFS, each running in both moderate (T159) resolution and high (T1279) resolution. The IFS has 91 vertical hybrid levels (top full level at 0.01 hPa) and thus should be categorized as a high-top atmospheric general circulation model. For the AMIP-type experiments, 47 continuous years were integrated from January 1961 to December 2007 with the observed history of sea surface temperature (SST) and sea ice fields, and fixed climatological radiative forcings. The AMIP integrations serve as the control experiment for the time-slice experiment. The time-slice integrations are also 47 years long, covering the period 2071–2117, but with the observed SST and sea ice conditions perturbed with monthly anomalies computed as the difference between 2065–2075 and 1965–1975 in the A1B scenario and historical simulations, respectively, using the Community Climate System Model [*Collins et al*., 2006]. The concentrations of greenhouse gases follow scenario A1B until year 2100; thereafter, concentrations are held constant at their 2100 values. Thus, contrasting the time slice against the AMIP simulations yields the climate change response of year 2070 relative to 1970 under the A1B scenario.

[8] In order to cross-check the results of the AMIP simulations, we also make use of the 13 month hindcast integrations started on 1 November of each of the years 1961–2007 for T159 and T1279. For each of the 47 integrations, the atmosphere is initialized with the ERA-40 (1961–1989) or ERA-Interim (1990–2007) conditions interpolated spatially to the resolution of the model. This set of simulations will be referred to as hindcast simulations.

[9] The primary data sets for evaluating the model performance of the AMs include the 40 year reanalysis of the European Centre for Medium-Range Forecast [*Uppala et al*., 2005] and the NCEP-DOE reanalysis-2 [*Kanamitsu et al*., 2002]. Unless noted explicitly, most of the comparison is against the estimation based on the ERA-40 reanalysis. The primary variable for the AM analysis is the six-hourly geopotential height data. To facilitate a direct comparison with the prior studies [e.g., *Gerber et al*., 2010], the six-hourly data are first converted to the daily mean before the analysis. For model data output, only selected pressure levels are available; thus, only 13 levels up to 10 hPa are used. The same levels from the ERA-40 reanalysis are employed for validation.

[10] The method for the AM calculation is similar to that of *Baldwin et al*. [2010] and *Baldwin and Thompson* [2009]. These studies defined the AMs separately for each pressure level as the leading empirical orthogonal function of the daily, deseasonalized, latitude-weighted, zonally averaged geopotential height anomalies poleward of 20° latitude in each hemisphere. Modifications were further made to this method following *Gerber et al*. [2010]: (i) the time series of the geopotential height anomalies were all detrended; (ii) to prevent global geopotential height fluctuations, which are unrelated to the zonal momentum structure, from aliasing onto the annular modes, the global mean geopotential of each day at each pressure level was subtracted. The autocorrelation function of the AM index and its *e*-folding time scale were then computed following *Baldwin et al*. [2003] with a Gaussian weighting (with a full width at half maximum of 60 days) applied to the daily time series. The time scale was estimated as the least squares fit of an exponential curve to the autocorrelation function cutoff at a 30 day lag.

3. Results

3.1. The Spatial Structure of the Annular Modes in the IFS AMIP Runs

[11] *Baldwin and Thompson* [2009] and *Gerber et al*. [2010] demonstrated that the annular mode accounts for over half the variance of the zonal flow at most levels in both hemispheres and provides an ideal multilevel metric for assessing the interaction between the troposphere and stratosphere. Observations show that there is an asymmetry between the two hemispheres in the fraction of variance of the tropospheric zonal wind explained by the annular mode: the value in the SH is higher than in the NH. This asymmetry is captured reasonably well by both resolutions (see Figure S1 in the supporting information). However, the IFS simulations still suffer the overestimation of the variance as most climate models do, although somewhat less so in T1279. The overestimation of the NAM variance is a bias commonly found in climate models [e.g., *Delworth et al*., 2006]. Increased resolution has some negative effects in addition to the benefits. For example, the SAM in T1279 accounts for too much variance in the stratosphere, and the minimum variance near the tropopause is too high in altitude compared to both ERA-40 and the T159 simulation (Figure S1b).

[12] The IFS shows considerable realism in simulating the meridional structure of the AM in both hemispheres. In the troposphere, the geopotential height pattern associated with the AM is characterized by a dipole, with the nodal point

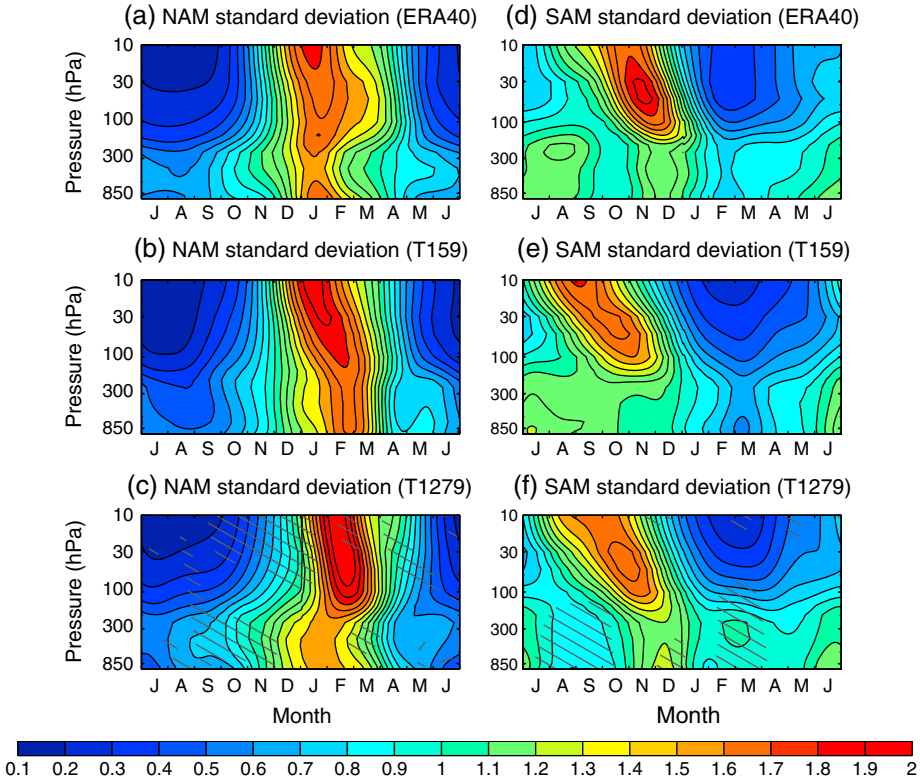

Figure 1. The standard deviation of the NAM and SAM indices as a function of season and pressure for (top) the ERA40 reanalysis and the IFS AMIP simulations at (middle) T159 and (bottom) T1279 resolutions. The hatching in the bottom panels indicates the areas where the difference of the standard deviation from the T159 case is significant at 10% confidence level based on *F* test.

indicating the peak of the anomalous westerly wind. At 100 hPa and above, the pattern elongates toward the equator, implying the associated geostrophic wind to be more monopolar in character, reflecting variation in the strength and size of the stratospheric polar vortex [*Gerber et al.*, 2010, Figure 4]. In the CMIP3 models, the nodal line and the peak equatorward of it are both displaced equatorward compared to their observational counterparts. Here, in both high- and moderate-resolution simulations, the meridional structure of the geopotential height of the AM is rather faithfully simulated with only ~1° latitude offset at most in the nodal latitude compared to the ERA40 (not shown).

3.2. Temporal Structure of the AMs in the AMIP Runs

[13] The seasonal and vertical structure of the annular mode variance is shown in Figure 1. The maximum occurs in the boreal winter for the NH and in the austral spring for the SH, a difference likely due to the more active stationary wave forcing and hence more active stratospheric sudden warming events in the NH and the dominance of the variability occurring during the time of vortex breakdown in the SH. The slant in isolines of the variance in the stratosphere is reasonably simulated by both resolutions, indicating descending AM variability. The T159 simulation misplaces the peak of the tropospheric NAM variance at late February, while the observed peak takes place in late January. The ~1 month delay in the T159 case is much alleviated with high-resolution simulation, and the improvement between late February and early March in the overestimation is significant (at 10% confidence level) based on *F* test. In the SH, the peak of the SAM variance in the stratosphere tends to occur about 1.5 months (1 month) too early in the T159 (T1279) simulation, and the rate at which the variability descends is too slow compared to ERA40. The early occurrence of the peak variance indicates that the final warming might occur too early in the model. Indeed, an inspection of the seasonal evolution of the polar cap temperature supports this speculation. The improvement due to high resolution is more visible in the SH troposphere; the T1279 AMIP simulation captures the November–December maximum, which is largely missing in the T159 simulation as in most CCMVal-2 models [*Gerber et al.*, 2010].

[14] Figure 2 shows the AM time scales as a function of altitude and season. The AM time scales in the stratosphere are consistently better in the IFS simulations than typical climate models, which show a tendency toward overestimation [*Gerber et al.*, 2010]. Similar to the typical climate models, the timing of the maximum persistence of the tropospheric NAM in T159 is delayed by a month or so compared to the reanalysis; this bias is somewhat ameliorated in the T1279 simulation. It is difficult to judge whether this improvement is the result of the better representation of the downward influence of the NAM from the stratosphere or the cross-scale interactions in the troposphere, since both the stratospheric and tropospheric processes can shape the seasonality of the AM time scales [*Simpson et al.*, 2011]. For the SH, the seasonality of the SAM time scale is also improved in the

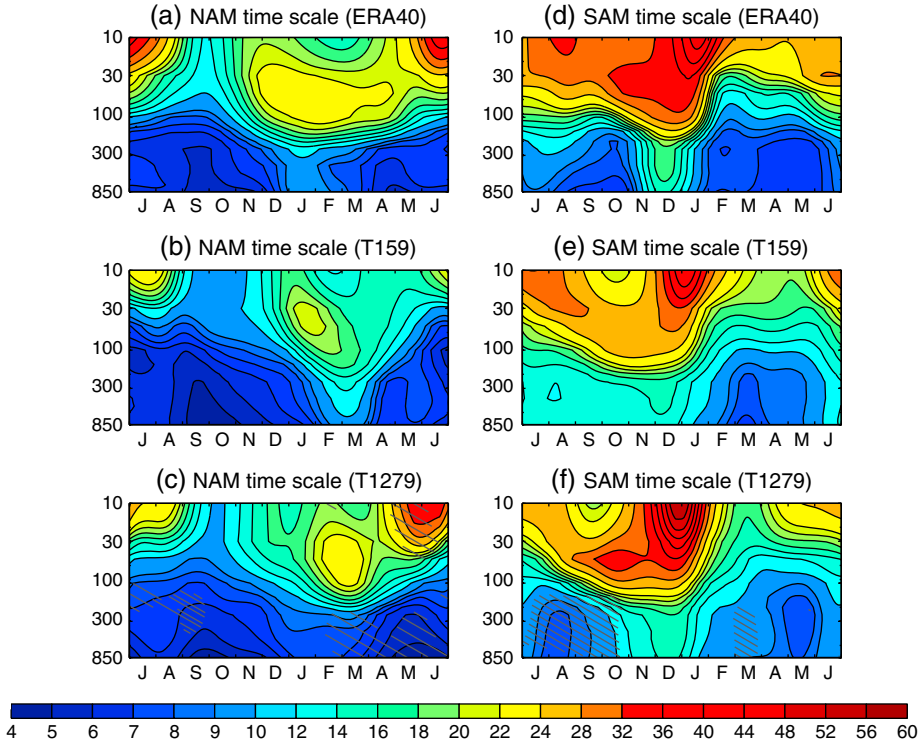

Figure 2. The *e*-folding time (days) of the NAM and SAM indices as a function of season and pressure for (top) ERA40 and IFS AMIP simulations at (middle) T159 and (bottom) T1279 resolutions. The hatching in the bottom panels indicates the areas where the difference of the AM time scale between the two resolutions is greater than the uncertainty of the time scale due to one standard deviation of the autocorrelation function of the AM index estimated following *Gerber et al*. [2008a, 2008b].

high-resolution simulation. In particular, the overestimation of the tropospheric time scales during the austral winter/spring in the moderate resolution, a feature likely related to the concomitant overestimation of the variance of the SAM in the troposphere, is much improved with the implementation of the high resolution. To get a sense about the significance of the change of the AM time scale due to the high resolution, we follow *Gerber et al*. [2008a, 2008b] to estimate the uncertainty of the time scale resulted from the internal variability of the autocorrelation function of the AM index, assuming that the AM index can be modeled as an AR(1) process. Hatching in Figures 2c and 2f highlights the areas where the value of the time scale in T1279 is outside the one standard deviation uncertainty range estimated from the T159 simulation.

[15] The same analysis was also performed with the hindcast simulations for T159 and T1279. The results for the variance and time scale analysis are shown in Figures S2 and S3, respectively. As in the AMIP run, T159 tends to simulate too late a peak in the annual evolution of the NAM variance and as a result places the maximum persistence of the tropospheric NAM in March. A similar delay in the peaking is also apparent in the tropospheric SAM variability in the T159 simulation. Although the improvement due to the high resolution is not as evident as the AMIP simulations, the tendency toward the alleviation of the bias of the delayed peaking is clear. We speculate that the phase bias in the T159 hindcast simulation is the result of the overestimation of the influence of the stratospheric final warming on the troposphere and the underestimation of that of the sudden warming. Extra caution should be used in interpreting the time scale analysis of the hindcast runs, since the time series for each year is truncated at November 30, leading to an artificial discontinuity and a dip in the persistence between November and December.

[16] To elucidate the connection between the biases in the lower stratosphere and the troposphere, we estimate the fraction of variance of the 30 day averaged 850 hPa index that can be explained by the antecedent daily index. This quantity, as a function of height and season, is the square of the correlation between the AM index on a particular day (day 0) and level, and the 31 day mean AM index (i.e., days 10–40) at 850 hPa with the former leading the latter by 10 days. The result (Figure 3) suggests that the lower stratosphere sometimes can be a better predictor for the near-surface annular mode index than the near-surface annular mode itself. This can be seen by the higher values of fraction of variance near the lower stratosphere at certain times during the year, for example, between November and January in the NH and between September and October in the SH. However, this stratosphere-originating predictability is hard to capture for models. In the NH, the IFS model tends to delay the season of the stratosphere-to-troposphere connection by 2 months compared to the reanalysis, seeming to echo the delayed maximum variance and persistence of the NAM index in the stratosphere. The lag correlation analysis of the T1279 simulation seems to capture a local maximum between November and December but is much weaker and 1 month too early than its reanalysis counterpart. Thus, in the NH, it appears that

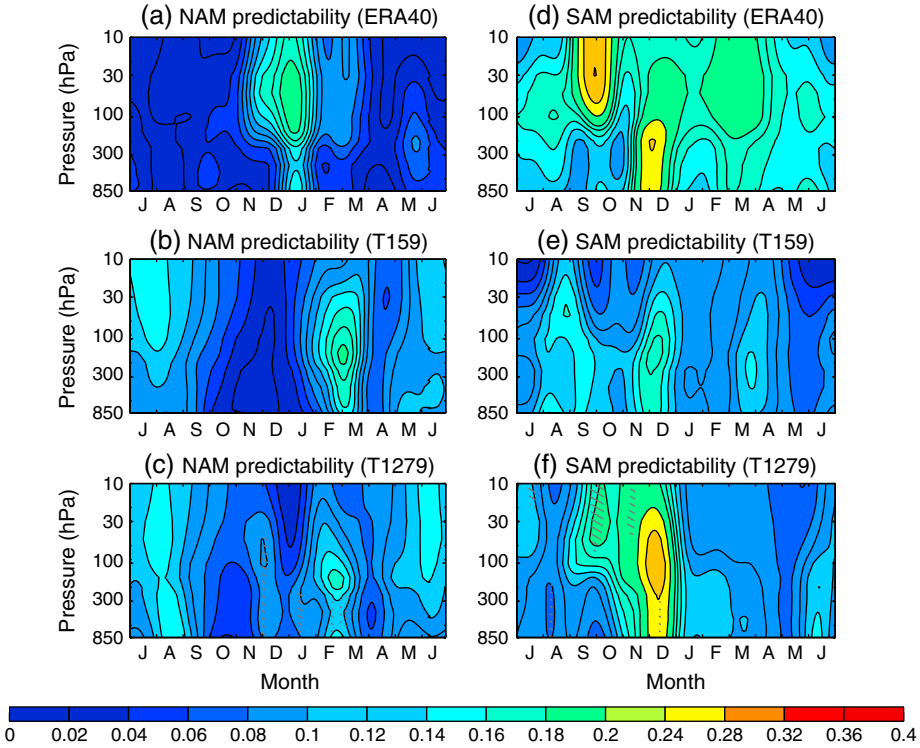

Figure 3. Same as Figure 2 but for the fraction of variance of the 31 day mean 850 hPa annular mode index, lagged by 10 days, that is linearly correlated with the instantaneous annular mode index as a function of season and pressure. Note that the observed estimate of the potential predictability is based on the NCEP-DOE reanalysis using data between 1979 and 2008. The hatching in the bottom panels indicates the areas where the increase of the explained variance relative to the T159 case is significant at 10% confidence level.

too much of the modeled potential predictability is associated with the final warming of the stratospheric vortex, as implied by the delayed maximum persistence of the NAM in both stratosphere and troposphere.

[17] Perhaps the most notable improvement due to the high resolution is in the predictability relationship between the September-October stratospheric SAM index and the near-surface SAM anomalies (compare Figures 3e and 3f). This, in conjunction with the ERA40 result (Figure 3d), suggests that the feature of the accentuated potential predictability during austral spring is real and not an artifact of instrumental changes or data assimilation algorithms. The significance of the change of the lagged covariance due to the T1279 resolution is further tested using a Fisher Z test, and the changes at the 10% confidence level are highlighted with hatching in Figure 3f. The T1279 simulation also captures the magnitude of the potential predictability near the tropopause level better, suggesting that at T1279 resolution, the IFS can have sizable potential skill in predicting the monthly mean tropospheric SAM index from its tropopause index with a lead of 10 days. Unfortunately, similar potential predictability remains elusive with the NAM, regardless of which resolution is used (two other resolutions, T511 and T2047, were also evaluated, but not shown).

3.3. Projecting the SH Westerly Shift

[18] In view of the modest but consistent improvements in the variance, time scale, and the downward connection of the SAM in the T1279 simulation relative to the T159 simulation, it may be more desirable to use the former for evaluating the future climate of the Southern Hemispheric westerly jet. Moreover, if the persistence of the tropospheric SAM in summer is augmented by the better captured downward influence from the stratosphere in the T1279 simulation (Figures 1f and 2f), one might expect it to project a greater shift of the SH westerly jet under global warming forcing if the SH summer westerly jet by any degree conforms to the fluctuation dissipation theorem. Figures 4a and 4b show the positions of the surface westerly jet, as a function of time of the year, in ERA40 (black line) and AMIP simulation with T159 (blue solid line in Figure 4a) and T1279 (green solid line in Figure 4b) resolutions and the corresponding time-slice experiments (dashed line). Both resolutions show similar seasonality in the projected poleward shift of the westerly jet, with a relatively larger shift during SH summer than winter. Additionally, it may not just be fortuitous that the T1279 time-slice run projects a greater shift than the corresponding T159 run during mid-summer when the SAM is more persistent in the T1279 than the T159 control simulations. It is of interest to note that increasing the horizontal resolution eightfold produces no appreciable shift in the mean position of the surface westerly wind but instead enhances the SAM persistence, in contrast to the sensitivity found with most of the climate models that the SH westerly jet in the higher-resolution models tends to be less equatorward biased and less persistent in its leading mode of variability, and responds in smaller magnitude to a same external forcing [*Gerber et al.*, 2008a, 2008b; *Kidston and Gerber*, 2010; *Barnes and Hartmann*, 2010].

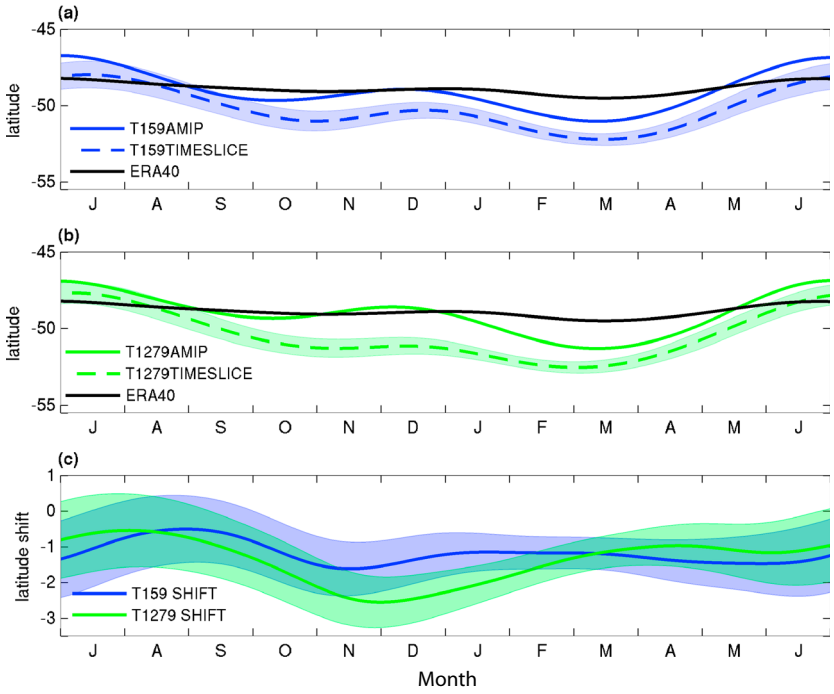

Figure 4. The mean locations of the surface westerly wind maximum in the SH from the AMIP (solid line) and time-slice (dashed line) simulations by the IFS at (a) T159 and (b) T1279 resolutions, together with the ERA40 reanalysis (black line). (c) The degrees of shift in the surface westerly winds in the time-slice simulations with T159 (blue line) and T1279 (green line) resolutions, respectively. The shading indicates the 95% confidence interval based on Welch's *t* test.

4. Concluding Remarks

[19] We assessed the main spatial and temporal characteristics of the annular modes and the associated downward stratosphere-to-troposphere influence in two sets of simulations using the ECMWF IFS model at T159 and T1279 resolutions, respectively. In general, the high-resolution version of the IFS model shows modest improvement relative to the modest resolution and typical climate models in simulating the main characteristics of the AMs, including the timing of the enhanced variability and persistence of the AMs, the marked asymmetry in the seasonality between the Northern and Southern Hemispheres, and the stratosphere-troposphere coupling during the active seasons. By comparing the seasonal structure of the AM variance in the stratosphere with the seasonality of the *e*-folding time of the AM index, it can be inferred that the stratospheric variability can exert notable impacts on the time scale of the tropospheric AMs. In agreement with *Gerber et al*. [2010], our analysis also showed that at a certain time of the season, the lower stratosphere is a better predictor for the phase of the AM events than the lower troposphere. In particular, the predictability stemming from the spring stratospheric condition in the SH is replicated in the higher-resolution model. In general, for most metrics examined, the high-resolution version of the IFS performs comparatively better than the moderate resolution.

[20] A note of caution should be added that some of the metrics (such as the time scale) examined here are quite sensitive to the choice of parameters and time period used in the calculation [e.g., *Simpson et al*., 2011], and a statistical significance test for the improvement is not readily available. To gain some confidence in the findings above, we repeated the same analysis for the 13 month hindcast simulations. A qualitatively similar delay is found in the seasonal evolution of the tropospheric NAM variance, time scale, and potential predictability in the T159 simulation, and the T1279 simulation tends to alleviate the bias toward delayed variability (see Auxiliary Figures S2 and S3). Given the complexity of the processes involved in determining the temporal characteristics of the AMs, it remains elusive to understand why simply increasing the horizontal resolution can help place the peak of the AM variability and persistence at the right time, a topic that is beyond the scope of this investigation.

[21] We can only speculate on the possible reason for the improvements in the T1279 runs as follows. The bi-harmonic diffusion used in IFS, which is scale selective, dissipates severely the high wave number range of the model-resolved power spectrum so as to distort the energy and enstrophy cascades at these scales. Indeed, significant difference was detected in the probability distributions of the finite-amplitude wave activity (personal communication, Abraham Solomon) and extratropical cyclones [*Jung et al*., 2011] between the T159 and T1279 simulations. The misrepresentation of the fine features of the potential vorticity filaments associated with these extreme events in T159 might result in some adverse rectification effect on the temporal characteristics of the AMs. All in all, the eightfold increase in the horizontal resolution can indeed bring about appreciable benefits.

[22] **Acknowledgment.** The authors acknowledge the careful reading and perceptive comments by two anonymous reviewers, who helped improved the quality of the manuscript substantially. JL is grateful to Edwin Gerber and Lantao Sun for their constructive discussion during the formative stage of this study. EP and JL are supported by NSF grant AGS-1064045. GC is supported by NSF grant AGS-1064079. NCEP-DOE Reanalysis 2 data was provided by the NOAA/OAR/ESRL PSD, Boulder, Colorado, USA, through web site http://www.esrl.noaa.gov/psd/.

[23] The editor thanks two anonymous reviewers for assistance evaluating this paper.

References

Baldwin, M. P., and T. J. Dunkerton (1999), Propagation of the Arctic Oscillation from the stratosphere to the troposphere, *J. Geophys. Res.*, *104*, 30,937–30,946, doi:10.1029/1999JD900445.

Baldwin, M. P., and T. J. Dunkerton (2001), Stratospheric harbingers of anomalous weather regimes, *Science*, *294*, 581–584.

Baldwin, M. P., and D. W. J. Thompson (2009), A critical comparison of stratosphere–troposphere coupling indices, *Q. J. R. Meteorol. Soc.*, *135*, 1661–1672.

Baldwin, M. P., D. B. Stephenson, D. W. J. Thompson, T. J. Dunkerton, A. J. Charlton, and A. O'Neill (2003), Stratospheric memory and skill of extended range weather forecasts, *Science*, *301*, 636–640.

Baldwin, M., et al. (2010), Effects of the stratosphere on the troposphere, in *SPARC Report on the Evaluation of Chemistry-Climate Models*, edited by V. Eyring, T. G. Shepherd, and D. W. Waugh, *SPARC Rep. 5, WCRP-132, WMO/TD-1526*, 379–412, World Climate Research Programme, Geneva, Switzerland.

Barnes, E. A., and D. L. Hartmann (2010), Testing a theory for the effect of latitude on the persistence of eddy-driven jets using CMIP3 simulations, *Geophys. Res. Lett.*, *37*, L15801, doi:10.1019/2010GL044144.

Chen, G., and R. A. Plumb (2009), Quantifying the eddy feedback and the persistence of zonal index in an idealized atmospheric model, *J. Atmos. Sci.*, *66*, 3707–3720.

Collins, W. D., et al. (2006), The Community Climate System Model version 3 (CCSM3), *J. Clim.*, *19*, 2122–2143.

Delworth, T. L., et al. (2006), GFDL's CM2 global coupled climate models-Part 1: Formulation and simulation characteristics, *J. Clim.*, *19*, 643–674.

Dirmeyer, P. A., et al. (2011), Simulating the diurnal cycle of rainfall in global climate models: Resolution versus parameterization, *Clim. Dyn.*, *39*, 399–418, doi:10.1007/s00382-011-1127-9.

Gerber, E. P., L. M. Polvani, and D. Ancukiewicz (2008a), Annular mode time scales in the Integovernmental Panel on Climate Change Fourth Assessment Report models, *Geophys. Res. Lett.*, *35*, L22707, doi:10.1029/2008GL035712.

Gerber, E. P., S. Voronin, and L. M. Polvani (2008b), Testing the annular mode autocorrelation time scale in simple atmospheric general circulation models, *Mon. Weather Rev.*, *136*, 1523–1536.

Gerber, E. P., et al. (2010), Stratosphere-troposphere coupling and annular-mode variability in chemistry-climate models, *J. Geophys. Res.*, *115*, D00M06, doi:10.1029/2009JD013770.

Jung, T., et al. (2011), High-resolution global climate simulations with the ECMWF model in the Athena Project: Experimental design, model climate and seasonal forecast skill, *J. Clim.*, *25*, 3155–3172.

Kanamitsu, M., W. Ebisuzaki, J. Woollen, S.-K. Yang, J. J. Hnilo, M. Fiorino, and G. L. Potter (2002), NCEP-DEO AMIP-II Reanalysis (R-2), *Bull. Am. Meteorol. Soc.*, *83*, 1631–1643.

Kidston, J., and E. P. Gerber (2010), Intermodel variability of the poleward shift of the austral jet stream in the CMIP3 integrations linked to biases in 20th century climatology, *Geophys. Res. Lett.*, *37*, L09708, doi:10.1029/2010GL042873.

Kinter, J. L., III et al. (2013), Revolutionizing climate modeling-Project Athena: A multi-institutional, international collaboration, *Bull. Am. Meteorol. Soc.*, *94*, 231–245.

Leith, C. E. (1975), Climate response and fluctuation dissipation, *J. Atmos. Sci.*, *32*, 2022–2026.

Manganello, J. V., et al. (2012), Tropical cyclone climatology in a 10-km global atmospheric GCM: Toward weather-resolving climate modeling, *J. Clim.*, *25*, 3867–3893.

Miller, R. L., G. A. Schmidt, and D. T. Shindell (2006), Forced annular variations in the 20th century Intergovernmental Panel on Climate Change Fourth Assessment Report models, *J. Geophys. Res.*, *111*, D18101, doi:10.1029/2005JD006323.

Ring, M. J., and R. A. Plumb (2008), The response of a simplified GCM to axisymmetric forcings: Applicability of the fluctuation-dissipation theorem, *J. Atmos. Sci.*, *65*, 3880–3898.

Simpson, I. R., P. Hitchcock, T. G. Shepherd, and J. F. Scinocca (2011) Stratospheric variability and tropospheric annular-mode timescales, *J. Geophys. Res.*, *111*, D18101, doi:10.1029/2011GL049304.

Son, S.-W., et al. (2008), The impact of stratospheric ozone recovery on the Southern Hemisphere westerly jet, *Science*, *320*, 1486–1489, doi:10.1126/science.1155939.

Thompson, D. W. J., and J. M. Wallace (2000), Annular modes in the extratropical circulation: Part I. Month to month variability, *J. Clim.*, *13*, 1000–1016.

Uppala, S. M., et al. (2005), The ERA-40 Re-Analysis, *Q. J. R. Meteorol. Soc.*, *131*, 2961–3012.